ACS SyntheticBiology

Research Article

pubs.acs.org/synthbio

MicroRNA-Based Single-Gene Circuits Buffer Protein Synthesis Rates against Perturbations

Timothy J. Strovas,[§,†] Alexander B. Rosenberg,[§,†] Brianna E. Kuypers,[†] Richard A. Muscat,[†] and Georg Seelig*[,†,‡]

[†]Department of Electrical Engineering and [‡]Department of Computer Science & Engineering, University of Washington, Seattle, Washington 98195-5852, United States

Supporting Information

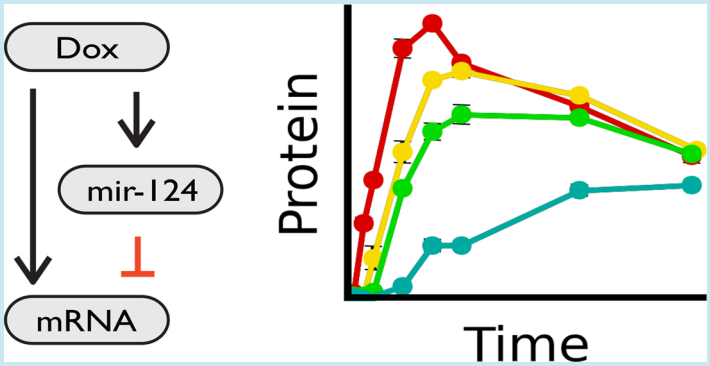

ABSTRACT: Achieving precise control of mammalian transgene expression has remained a long-standing, and increasingly urgent, challenge in biomedical science. Despite much work, single-cell methods have consistently revealed that mammalian gene expression levels remain susceptible to fluctuations (noise) and external perturbations. Here, we show that precise control of protein synthesis can be realized using a single-gene microRNA (miRNA)-based feed-forward loop (sgFFL). This minimal autoregulatory gene circuit consists of an intronic miRNA that targets its own transcript. In response to a step-like increase in transcription rate, the network generated a transient protein expression pulse before returning to a lower steady state level, thus exhibiting adaptation. Critically, the steady state protein levels were independent of the size of the stimulus, demonstrating that this simple network architecture effectively buffered protein production against changes in transcription. The single-gene network architecture was also effective in buffering against transcriptional noise, leading to reduced cell-to-cell variability in protein synthesis. Noise was up to 5-fold lower for a sgFFL than for an unregulated control gene with equal mean protein levels. The noise buffering capability varied predictably with the strength of the miRNA-target interaction. Together, these results suggest that the sgFFL single-gene motif provides a general and broadly applicable platform for robust gene expression in synthetic and natural gene circuits.

KEYWORDS: *adaptation, noise, microRNA, feed-forward loop*

Gene circuits are subject to sudden changes in their environment and random fluctuations in the numbers of their components ("noise").[1] For example, a reporter gene integrated into the genome of a mammalian cell was shown to be transcribed in bursts, resulting in a wide range of mRNA and protein molecule numbers across a population of cells.[2] Such randomness is sometimes exploited in cellular decision-making but also poses a challenge to the reliability of biological and engineered gene circuits.[3−5] In order to make synthetic gene circuits practically useful for tissue engineering, cellular reprogramming and related fields that require the long-term stable expression of engineered genetic programs in mammalian cells, we need to develop methods for reliably buffering transgene expression against both global perturbations and transcriptional noise.

Mounting evidence points to an important role for miRNA, a widespread class of posttranscriptional repressors,[6] in buffering biological gene circuits against disturbances.[7−9] For example, a miRNA embedded in an incoherent feed-forward loop (IFFL) has been shown to ensure correct eye development in drosophila embryos exposed to temperature fluctuations.[10] A miRNA-based approach to engineering robust gene circuits is appealing because expression constructs for miRNA of arbitrary sequence are readily available,[11] and target sites for any miRNA can be inserted into an mRNA of interest.[12] This flexibility has been exploited in the design of a variety of RNA-based synthetic mammalian gene circuits.[13−17] The high degree of modularity also means that miRNA-based approaches to gene

Received: November 21, 2013
Published: January 15, 2014

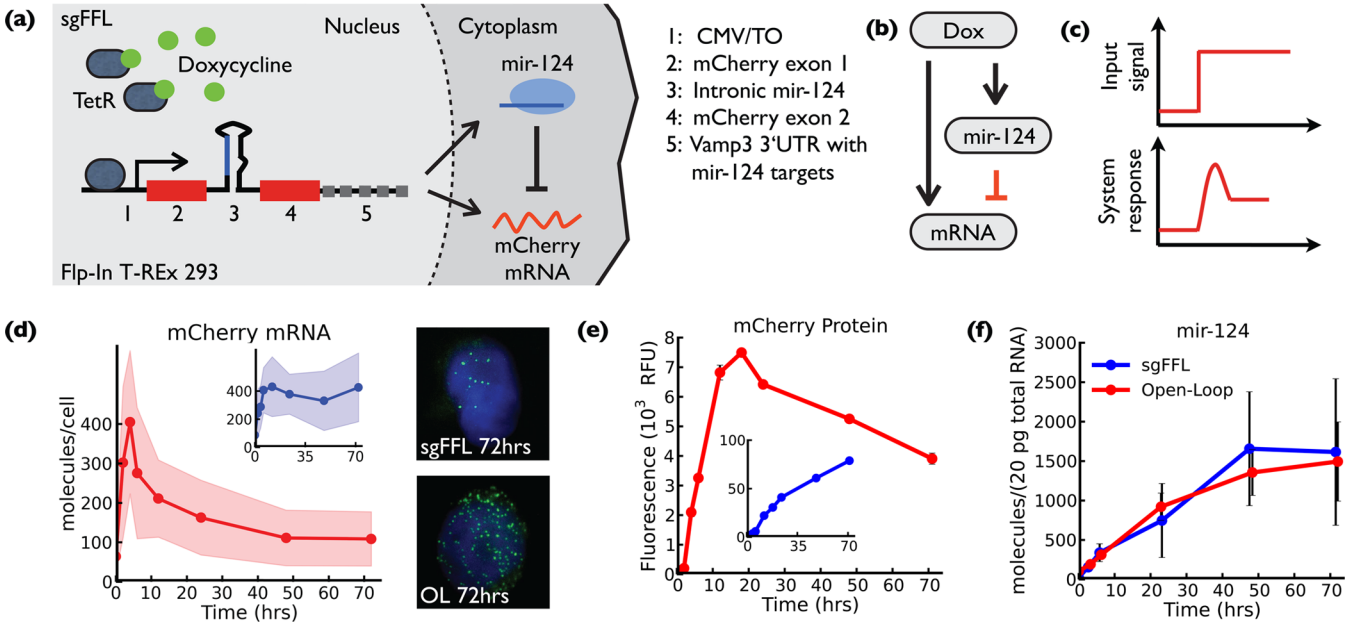

Figure 1. miRNA-based single-gene circuit can generate transient pulses in gene expression. (a) Induction of the sgFFL cell line by Dox results in transcription of a pre-mRNA containing the primary mir-124 and the mCherry coding sequence. The mature mir-124-RISC complex then targets the 3′UTR of the mCherry transcript. The mir-124 targeted 3′UTR was deleted in the open-loop cell line. (b) The miRNA expression construct implements an incoherent feed-forward motif. (c) The sgFFL exhibits transient pulse generation and adaptation in response to a sustained change in the level of the upstream regulator. (d) The sgFFL mCherry mRNA shows a pronounced pulse around t = 5 h (red). No peak is observed in the control cell line (inset, blue). Data was obtained using single molecule FISH and both mean and variance are indicated. Representative images for the two cell lines at the 72 h time point are shown. (e) A pulse is also clearly visible in the expression of the mCherry protein in the sgFFL line but not in the control (inset). Protein expression was assayed using flow cytometry (RFU, relative fluorescence unit). (f) RT-qPCR data show similar accumulation of miRNA for the sgFFL and control cell lines.

expression buffering may be easily adapted to different regulatory contexts.

Theoretical work supports the notion that the microRNA-based IFFL architecture, in which an upstream transcription factor simultaneously activates expression of a mRNA and of a miRNA targeting that same mRNA, is well suited for limiting variability in gene expression.[8,18] Furthermore, IFFLs can exhibit adaptation;[19−21] that is, they respond to a sustained change in the level of a stimulus with a transient gene expression pulse before resetting to the original prestimulus expression level. Adaptation provides a mechanism for buffering steady state gene expression against global perturbations while transiently propagating information about that perturbation.

The sgFFL architecture, in which an intronic miRNA targets the mRNA from which it originates, forms a compact, single-gene implementation of an IFFL making it an attractive target for engineering low-noise transgenes.[22] Recent work using transient plasmid transfections showed that a sgFFL can buffer gene expression against cell-to-cell variability in plasmid copy number.[16] However, it remains unclear how noise buffering in a sgFFL architecture is achieved at the single-copy level, how populations can adapt to time-varying perturbations, or if the steady state protein levels may be predictably tuned.

We engineered a family of sgFFL variants with different biochemical parameters and integrated the constructs into the genome to create stable cell lines. Genomic integration allowed us to quantify miRNA, mRNA, and protein dynamics over extended time periods and made it possible to characterize steady state gene expression noise without confounding factors due to plasmid copy number variations. We found that this network achieved biochemical adaptation and was effective in buffering against transcriptional noise, leading to reduced cell-to-cell variability in protein synthesis. We varied the number and type of miRNA target sites as well as the miRNA production levels and showed that steady state levels can be tuned with buffering increasing for stronger interactions. Together, our results suggest that the sgFFL mechanism provides a robust and modular mechanism for buffering gene expression against perturbations.

RESULTS AND DISCUSSION

Adaptation in a Single-Gene Network. We built a synthetic autoregulatory gene circuit by inserting an intron containing the mouse mir-124−3 gene into a red fluorescent reporter (mCherry). The pre-mRNA is transcribed from a doxycycline (Dox)-inducible promoter (CMV/TO), leading to coexpression of mir-124 and mCherry[23] (see Figure 1a). To create a repressive regulatory link between the miRNA and the mCherry transcript, we added a truncated version of the mir-124-regulated 3′UTR of the *Vamp3* gene to the mRNA.[24] This 3′UTR contains one 6-mer and three 7-mer target sites complementary to the mir-124 seed region (nucleotides 2−8 from the 5′ end of the miRNA). To better observe the dynamics of gene expression, we destabilized the mCherry protein using a standard PEST degradation tag. A stable cell line was created by genomic integration of the circuit into a Flp-In T-REx 293 cell line that expresses a constant background of the TetR repressor protein. By tightly binding to TetR and relieving its repressive activity, Dox acts as an activator for both the mCherry mRNA and mir-124. The corresponding network diagram is shown in Figure 1b with the negative regulatory link highlighted in red. We also engineered a control cell line containing an expression construct without the target-

dx.doi.org/10.1021/sb4001867 | ACS Synth. Biol. 2014, 3, 324−331

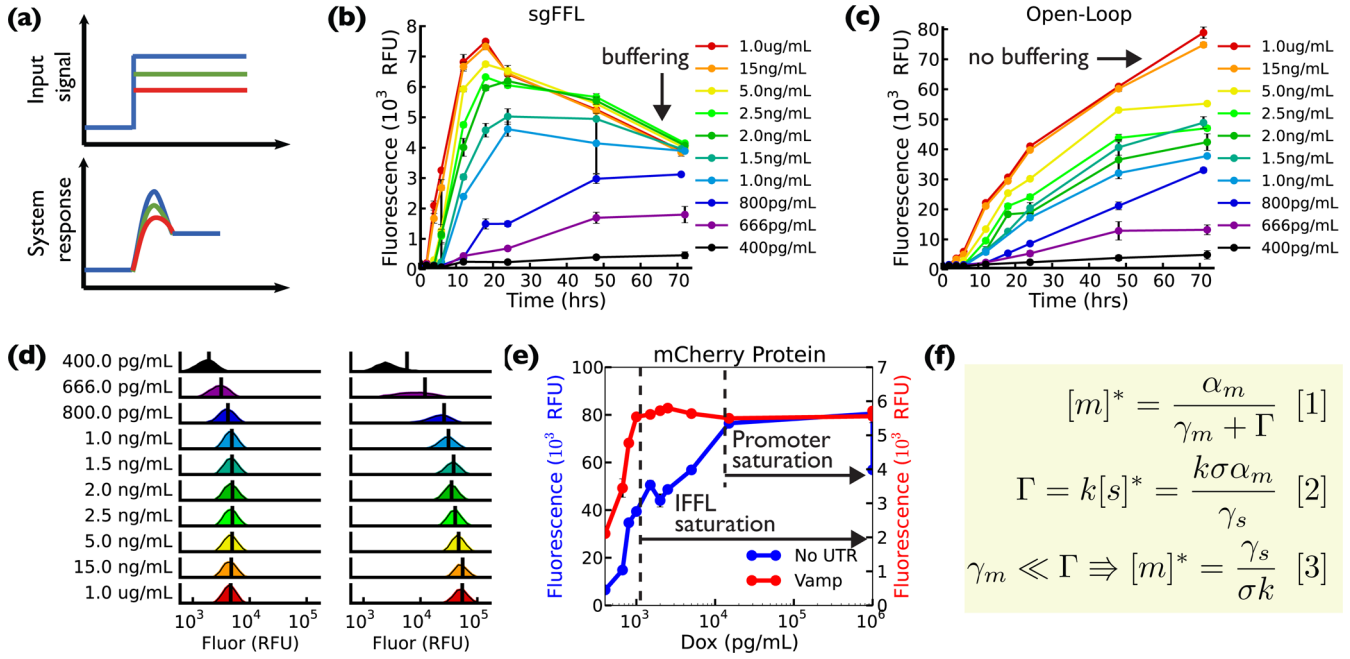

Figure 2. miRNA-based sgFFL buffers gene expression against a sustained external stimulus. (a) In an adaptive gene circuit steady state protein expression levels are independent of the input amplitude. However, the pulse is proportional to the input. (b) Varying levels of Dox induction lead to distinct peak amplitudes that converge to the same steady state level. (c) No steady state buffering or pulsing is observed in the open loop control cell line. (d) Fluorescence histograms for the sgFFL (left) and control cell line (right) at different levels of induction. Data was taken 72 h after induction and 30 000 cells were used in each experiment. Means are indicated with a black line. (e) Mean fluorescence at 72 h as a function of Dox. The open loop control cell line can reach higher fluorescence levels at full induction, but the sgFFL cell line reaches its maximal fluorescence at lower promoter activities. (f) Buffering can be understood from a simple steady state model of gene expression (see Supporting Information, supplementary text for details). $[m]^*$ is the steady state levels of the mCherry mRNA (eq 1). The mRNA production rate is α_m and the miRNA production rate is $\sigma\alpha_m$. Here, σ accounts for different production efficiencies of the mRNA and miRNA. The native mRNA degradation rate is γ_m, the miRNA degradation rate is γ_s, and Γ is the degradation rate of the mRNA due to the miRNA, which is proportional to $[s]^*$, the steady state amount of the miRNA (eq 2). As mRNA degradation due to the miRNA becomes the main source of degradation ($\Gamma \gg \gamma_m$), the steady state levels of mRNA become independent of the production rate α_m (eq 3).

containing Vamp3 3′UTR, referred to as open-loop control. Plasmid maps for both cell lines are shown in Supporting Information Figure S1.

Sustained activation of the sgFFL with Dox led to a transient pulse in gene expression (Figure 1c,d). A sharp peak in mRNA levels as measured by single-cell RNA FISH[2] was observed around 5 h after induction (Figure 1d), before mRNA levels (72 h time point) returned close to their prestimulus value. The measured mRNA dynamics display near perfect adaptation, a behavior compatible with feed-forward loop architectures.[19−21] Protein expression was measured by flow cytometry and followed a similar course to the mRNA expression (Figure 1e). Unlike the mRNA, which is actively targeted by the miRNA, proteins are only slowly cleared from the cell resulting in a slow poststimulus decay of fluorescence. No pulse was seen in the mRNA or protein levels in the open-loop control cell line. Instead, protein and mRNA both monotonically increased toward their respective steady state values (insets, Figure 1d,e).

We used quantitative PCR to directly measure the levels of mature mir-124. MiRNA levels in the sgFFL and open-loop control cells were almost identical and, over the course of the experiment, gradually approach steady state without pulsing (Figure 1f). The slow approach to steady state is primarily due to the high stability of the RISC-bound miRNA. Furthermore, the similarity in the miRNA levels for the sgFFL and control cell lines implies that mRNA targeting does not dramatically accelerate miRNA turnover.[25] To confirm that the repression of mCherry is in fact due to the miRNA rather than competition for cellular resources or other nonspecific effects, we transfected sgFFL cells with a LNA-modified antisense oligonucleotide complementary to mir-124. Antisense transfection restored red fluorescence confirming direct repression of the target by the miRNA (Supporting Information Figure S2). We further confirmed this result by engineering a stable sgFFL cell line where we deleted the primary miRNA from the intron. This cell line did not show pulsing and behaved similar to the original open-loop control cell line (Supporting Information Figure S3).

Gene Expression Buffering. The steady state levels in an ideal adaptive system should be insensitive to the size of the stimulus (Figure 2a). To explore if this is true for the sgFFL, we performed experiments in which we systematically varied the level of induction using Dox (Figure 2b,c). We identified a regime of Dox concentrations that resulted in intermediate promoter activities as evidenced by the variations in initial rates and peak heights. Traces that were clearly distinct at the peak converged to the same, subpeak steady state level (Figure 2b). For example, induction with 1−15 ng/mL Dox led to different initial rates and pulse amplitudes but very similar steady states. Such convergence of traces corresponding to different promoter activities is not seen in the time-course data for the control cell line. Instead, initial differences were amplified over the course of the experiment and resulted in clearly distinct end points (Figure 2c). We note that the maximal mean fluorescence achievable in the sgFFL cell population is lower than is the case for the open-loop control cell line, because at

dx.doi.org/10.1021/sb4001867 | ACS Synth. Biol. 2014, 3, 324−331

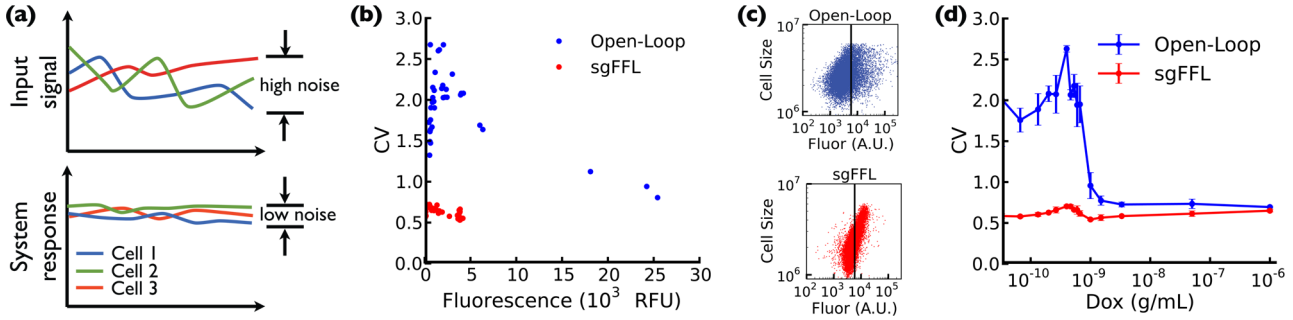

Figure 3. Single-cell analysis reveals noise suppression in a sgFFL. (a) The sgFFL motif is predicted to buffer the expression of the target gene against variability in the upstream regulator. (b) Each data point in the plot corresponds to the fluorescence mean and coefficient of variation of the fluorescence distributions shown in Figure 2d. All data were collected 72 h after cells were induced with varying amounts of Dox. At the same mean, the noise in the sgFFL cell line is up to 5-fold lower than in the control. (c) Each data point corresponds to a single cell from a population of genetically identical cells. Cell size (forward scatter) is plotted against fluorescence. Black lines indicate mean fluorescence. At any given cell size, the distribution of fluorescence values is narrower for the sgFFL cells. (d) Noise for sgFFL and open loop control cell lines plotted against the concentration of Dox. Noise is lower in the sgFFL cell line for all Dox levels.

the highest level of induction the miRNA has a substantial repressive effect.

In most of our experiments, we follow the system dynamics over a three-day period. However, we note that the system has not completely reached steady state at the 72 h time point and some residual fluorescent protein from the transient peak remains in the cells. We thus also ran an extended 120 h time course experiment with the sgFFL cell line and using several different Dox concentrations (Supporting Information Figure S4). These longer time course experiments agree with the findings shown in Figure 2 and suggest that all dynamics relevant to gene expression buffering can be observed within three days.

Figure 2d,e summarizes the results on gene expression buffering by comparing the steady state expression levels of the control and sgFFL data as a function of Dox concentration. This analysis again clearly shows that steady state protein expression saturates and becomes insensitive to promoter activity before the promoter is fully active. The observed gene expression buffering can be understood from a model that compares RNA production and degradation rates (see Figure 2f and Supporting Information, supplementary text and Figure S5): the mRNA steady state level is determined by the ratio of the mRNA production and degradation rates, with both miRNA-induced and miRNA-independent processes contributing to the degradation rate. In the sgFFL, the production rates of the mRNA and miRNA are proportional to one another such that an increase in the mRNA production is always accompanied by an increase in miRNA production and, consequently, in an increase in miRNA-induced degradation. Thus, steady state mRNA levels become independent of the mRNA production rate if the rate of mRNA degradation due to the miRNA is large compared to the native rate of mRNA degradation.

Noise Suppression. How is buffering manifested at the single cell level? Cell-to-cell variability in TetR expression, Dox uptake, and other biochemical parameters naturally creates a range of promoter activities even among genetically identical cells in the same environment (Figure 3a).[4] This randomness results in a distribution of the experimentally measured fluorescence values in a population of cells (e.g., Figure 2d). We used the coefficient of variation (CV, standard deviation divided by the mean) of the fluorescence distribution as a measure for the biochemical noise. Figure 3d shows the CV as a function of the mean fluorescence for the control and sgFFL cell lines. Intriguingly, if we compare populations with the same mean, we find that the noise for the sgFFL line is up to 5-fold lower than noise for the control cell line, suggesting that the sgFFL network architecture acts as a buffer against variability in an upstream regulator. This point is stressed by the scatter plots in Figure 3c showing two cell populations with similar mean fluorescence: we found that the range of fluorescence values in the sgFFL population is considerably narrower than in the control population at any given cell size.

To achieve the same mean fluorescence in a population of sgFFL and open-loop control cells, it was necessary to more strongly induce the sgFFL. It is tempting then to assume that noise suppression is simply the result of comparing two processes corresponding to different underlying promoter activities. In that case, it is expected that noise should be lower for the more transcriptionally active promoter.[26] However, while this mechanism contributes to the observed effect it does not appear to be the only reason for noise reduction in the sgFFL cell line. In fact, we note that noise was lower in the sgFFL cell line than in the open loop control even when compared at the same level of promoter induction (Figure 3d).

Finally, we observed that for both cell lines noise is highest for Dox concentrations corresponding to intermediate fluorescence values (Supporting Information Figure S6). This is not surprising since in this regime small differences between cells are amplified by the strong nonlinearity of the promoter response function. Similar results have previously been reported in the literature.[27] At all levels of induction, the CV values measured in our experiments are in the range of values previously reported for endogenous proteins in mammalian cells.[28]

Tuning Network Parameters by Varying the Number of Binding Sites, Interaction Type, and miRNA Number. Next we set out to demonstrate that adaptation and noise suppression can be observed over a range of biochemical network parameter values. Following ref 24, we eliminated either one or two 7-mer seed target sites from the Vamp3 3′UTR and then generated sgFFL expression systems and cell lines sgFFLΔ3 and sgFFLΔ23 based on these modified 3′UTRs (see Figure 4a and Supporting Information Figure S1). The steady state analysis in Figure 4b shows that buffering is observable in sgFFLΔ3 and sgFFLΔ23. Figure 4c

dx.doi.org/10.1021/sb4001867 | ACS Synth. Biol. 2014, 3, 324−331

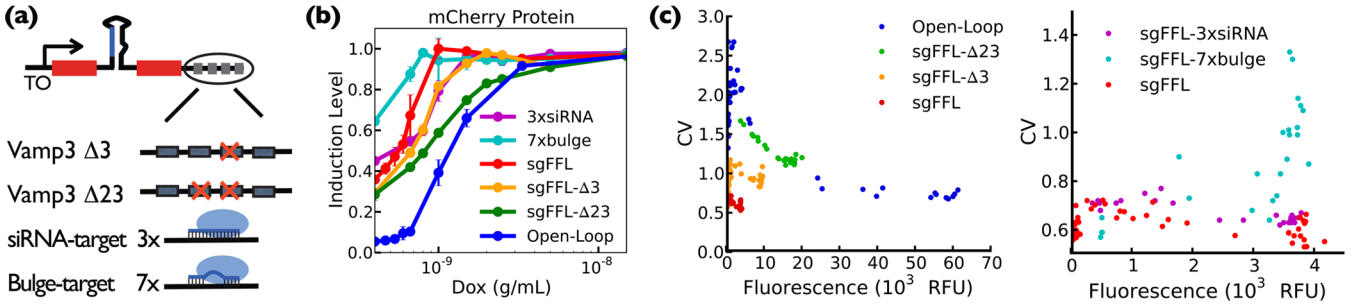

Figure 4. Buffering is tunable by changing the strength of the interaction between miRNA and target. (a) One and two mir-124 seed sites were deleted in the sgFFL-Δ3 and sgFFL-Δ23 cell lines. The 3′UTRs of sgFFL-3xsiRNA and sgFFL-7×bulge were built with three siRNA-like targets (fully complementary to mir-124) and seven bulge targets (fully complementary except central three nucleotides), respectively. (b) Mean fluorescence at 72 h as a function of Dox for all cell lines including open-loop control and sgFFL. The fluorescence for each cell line is normalized to the respective maximal induction levels. All sgFFL cell lines reach their maximal fluorescence at lower promoter activities than the control, indicative of a buffering effect. The most pronounced buffering is observed with the seven bulge targets. Buffering becomes less pronounced as interactions become weaker. Full time-course data for all cell lines is shown in Supporting Information Figure S7. (c) Noise is lower in any of the sgFFL cell lines than in the control. Noise reduction becomes more pronounced with increasing strength of interactions, except for the sgFFL-7×bulge line, which exhibits comparably high variability.

demonstrates that noise is suppressed compared to the control in both sgFFL mutant cell lines. Supporting Information Figure S7 shows time-course flow cytometry data for these constructs; protein expression pulsing becomes weaker with decreasing number of target sites and steady state levels are inversely correlated to the number of targets (Figure 4b). As expected from our model, buffering becomes less pronounced with decreasing strength of the interactions but is observable over a range of parameter values.

To investigate if adaptation and buffering are observable with different types of miRNA targets and interaction mechanisms, we also created sgFFL constructs with synthetic 3′UTRs that contained either three siRNA-like or seven bulge target sites (Figure 4d, Supporting Information Figures S1 and S9). The corresponding stable cell lines are sgFFL-3×siRNA and sgFFL-7×bulge. In the siRNA-like constructs, the sites are fully complementary to the miRNA, which results in cleavage of the mRNA target by the miRNA-RISC complex. In bulge constructs, the targets are fully complementary except for the central three nucleotides of the miRNA, which inhibits catalytic cleavage but still provides very strong interactions between miRNA and mRNA.[29] In agreement with our model (Figure 2f), these strong interactions lead to very clear signatures of adaptation in the time-course data (Supporting Information Figure S7) and result in strong noise suppression (Figure 4b,c). However, we note that noise is higher in the sgFFL-7×bulge cell line than either the sgFFL or sgFFL-3×siRNA cell lines (Figure 4c), even though buffering is very pronounced at the level of the population mean (Figure S7c). In previous work,[29] synthetic mRNAs with multiple bulge targets have been used as "sponges" for binding and inhibiting endogenous miRNAs. We speculate that we observe a similar effect here: given the very large number of potential target sites it is possible that in some cells all miRNA are bound to only a subset of the available mRNA targets, meaning that other mRNA can escape regulation resulting in increased variability.

We next asked if increasing the miRNA production rate could have a similarly pronounced effect on adaptation and buffering as increasing the number of miRNA targets, as would be expected from our model (Figure 2f). To increase the production rate of the miRNA without changing the production rate of the mRNA, we generated an sgFFL variant where two copies of the same primary microRNA were inserted into the intron (Supporting Information Figure S8). RT-qPCR data for the miRNA confirm the increase in miRNA production (Figure S8). The flow cytometry data show an earlier and lower-amplitude peak in protein expression, consistent with increased miRNA production (Figure S8). Furthermore, protein steady state levels are reduced as expected given the higher steady state concentration of miRNAs. Together, these results confirm that we can predictably tune steady state levels as well as the degree of buffering.

Multiple naturally occurring instances of the sgFFL motif have been experimentally identified[30−32] and several more have been predicted computationally,[22,31] suggesting an important role for this motif in biology. Thus, our results on disturbance rejection not only demonstrate that the sgFFL architecture forms a broadly useful tool for buffering transgenes against perturbations but also that it could provide a mechanism for stabilizing protein expression in biological gene circuits.

We also expect our results on noise suppression to apply to a broader class of endogenous miRNA-based IFFLs where the miRNA and target gene are expressed as independent transcriptional units,[10,33−35] if noise affecting the two promoters is correlated.[36] This will be the case, for example, for variations in transcription factor concentration or activity. Conversely, if two promoters are subject to uncorrelated noise, we would not expect to observe noise suppression. Importantly, however, adaptation and buffering against global perturbations should be observable independently of the exact arrangement of regulatory elements at the DNA level and may, in fact, be the most important biological role for this motif.

Given the slow degradation rate of the miRNA,[37] the sgFFL has fundamental limits on the types of noise it can filter. Perturbations in a cell that occur over long time scales, for example the accumulation of excessive TetR or global transcription factors, will be effectively filtered since the miRNA has time to compensate. However, perturbations that occur on the time scale of hours rather than tens of hours or days, will not be completely filtered, because the miRNA levels cannot change fast enough to compensate against resulting changes in transcription.

We found that the pulse amplitude for all adaptive sgFFLs is proportional to the size of the perturbation even though the steady state is buffered against that same perturbation. These different behaviors are apparent in Supporting Information

dx.doi.org/10.1021/sb4001867 | ACS Synth. Biol. 2014, 3, 324−331

Figure S9, which compares protein expression near the pulse maximum to the steady state. By multiplexing responses across different time frames, this circuit can thus buffer gene expression without losing information about the input signal. In spite of its simplicity, similar endogenous network motifs could serve to protect the current cell state against sudden changes in the environment while simultaneously activating new gene expression programs that enable cells to more permanently adapt to large environmental changes.[38]

How does our system compare to other mechanisms for noise reduction such as autoregulatory feedback?[27,39] Although feedback provides similar levels of noise suppression, the input-output characteristics of the promoter transfer function are very different. Autoregulatory feedback linearizes the promoter response function, and the rate of transcription is directly proportional to the size of the stimulus. In contrast, the sgFFL shows an all-or-none behavior with a rapid transition from the OFF to the ON state. Furthermore, for a wide range of promoter activities, transcription is independent of the levels of induction. These observations suggest different and complementary regulatory roles for these mechanisms.

In conclusion, we here quantitatively characterized a simple and modular mechanism for buffering transgenes in mammalian cells against perturbations. In combination with recent work on measuring and characterizing miRNA levels and interaction parameters in cells (see, e.g., refs 25, 40, and 41) our results suggest a path toward the rational design of complex molecular circuits with controlled temporal behaviors that are stably integrated and work reliably in mammalian cells. Engineered molecular circuits that use miRNAs as inputs and network components[13,14,17] could thus eventually become an engineering technology with applications that range from gene therapy to the control of differentiation in stem cells.

METHODS

Plasmids. Complete plasmid maps and sgFFL motif details are shown in Supporting Information Figure S1. Plasmids will be made available through Addgene.

Cell Culture. To improve cell adhesion, all culture dishes were coated with extracellular matrix (ECM) gel from Engelbreth−Holm−Swarm murine sarcoma (SigmaAldrich) diluted with α-MEM media (Mediatech) 1:200 for 16−24 h then rinsed with 1× Dulbecco's Phosphate Buffered Saline (DPBS; Mediatech) immediately before cells were plated. Cells were cultured in α-MEM media supplemented with 10% Tet System Approved fetal bovine serum (FBS; Clontech), penicillin (100 IU/ml; Invitrogen), streptomycin (100 μg/mL; Invitrogen), and L-glutamine (292 μg/mL; Invitrogen).

Selection of Stable Cell Lines. Transgenic strains were made in the Flp-In T-REx 293 cell line. The day before transfection, 1.5 million cells per well were seeded into a 6-well plate. pcDNA5 plasmid (8 μg) with 72 μg of pOG44 plasmid were transfected using Lipofectamine 2000 (Invitrogen) according to the manufacturer's protocol. Growth media was replaced 8 h post-transfection. Transfected cells were harvested in 1 mL 0.25% Trypsin-EDTA 48 h post-transfection and replated at 1:5, 1:10, and 1:50 dilutions in α-MEM media supplemented as previously described with the addition of Blasticidin (15 μg/mL; Invivogen) and Hygromycin B (100 μg/mL; Invivogen). Media with Blasticidin and Hygromycin was replaced 3 days and 7 days post-transfection. Once visible, 10−17 days post-transfection, individual colonies were dislodged in 250 μL 0.25% Trypsin-EDTA and moved into a 24-well plate, expanded, screened for phenotype, and propagated for this study.

Time-Course Experiments. Cells were seeded into ECM-coated 24-well plates, at a density of 50 000 cells per well, approximately 73 h prior to collection. During the period between seeding and collection, cells were maintained in α-MEM media supplemented as above. Wells were induced, in duplicate, at 72, 48, 24, 18, 12, 6, 4, 2, and 0 h before collection by the addition of doxycycline hyclate (Dox, stock concentration: 20 μg/μl). For collection, cells were harvested 12 wells at a time by first aspirating growth media, followed by addition of 100 μL 0.25% Trypsin-EDTA (Invitrogen) and resuspension in 250 μL 1× DPBS with 2% (v/v) FBS. Cells were strained through a 40 μM filter before flow cytometry. For each reaction condition, a population of 30 000 cells was collected and analyzed on an Accuri C6 flow cytometer.

mRNA and miRNA Quantitative RT-PCR. Total RNA was purified using the miRNeasy kit (Qiagen) and 20 units of SUPERase-In (Applied Biosystems) was added to both the on column DNase reactions and the final purified total RNA. RNA concentrations were measured using a NanoDrop spectrophotometer (Thermo Scientific); 260/280 nm ratios were consistently greater than 1.8, and RNA integrity was spot-checked using native agarose gels. Reverse transcription reactions were conducted using the Taqman microRNA Reverse Transcription Kit scaled to a 22.5 μL volume with Taqman microRNA Assay reverse transcription primers (for miRNA; Applied Biosystems) and Oligod(T)23 VN primers (for mRNA). Quantitative PCR was conducted on a CFX96 real-time PCR machine using SsoFast EvaGreen (mRNA) and Probes (miRNA) Supermixes (Biorad) following manufacturer protocols. RNA was detected using Taqman microRNA Assays (miRNA; Applied Biosystems) and primers specific to mCherry (Fwd, GGCTTCAAGTGGGAGCGCGT; Rev, GCATTACGGGGCCGTCGGAG; IDT) and TBP (Fwd, CACGAACCACGGCACTGATT; Rev, TTTTCTTGCTGCCAGTCTGGA; IDT). Data were normalized using uninduced samples, TBP[42] and hsa-mir-9*[43] as controls with the $\Delta\Delta$Ct method.[44] hsa-mir-124, hsa-mir-9*, mCherry, and TBP qPCR reactions had efficiencies of 95.9%, 101.9%, 87.9%, and 88.3%, respectively.

Single-Molecule FISH. A FISH probe set,[2,45] consisting of 48 oligonucleotides complementary to the exons coding mCherry and H2B, was designed using Stellaris Probe Designer software. The probe set was synthesized by the manufacturer (Biosearch Technologies, CA) labeled with the far-red fluorophore Quasar 670 (similar to Cy5). Cells were prepared for imaging using a modified version of the manufacturers guidelines for cells in suspension. Trypsinized cells were fixed, permeabilized and stored at −20 °C. Probes, incubated overnight at a concentration of 125 nM, were hybridized to target mRNA in a 20% formamide hybridization solution. Cells were imaged in Vectashield solution (Vecta Laboratories, CA) to minimize photobleaching. Z-stacks were taken across the entirety of the cell on a Nikon Ti Eclipse, with 100× objective and CoolSnapEZ camera. Images were analyzed using SpotFinding Suite.[46] A manually curated training set of "true" spots was used to determine the fitting parameters to identify unclassified candidate spots.

LNA Transfections. In a 24-well plate, fully induced sgFFL cells were transfected with 10 nM LNA (Exiqon) using RNAiMAX (Invitrogen) according to the manufacturer's protocol.

■ ASSOCIATED CONTENT

Supporting Information

Supplemental text and additional figures as described in the text. This material is available free of charge via the Internet at http://pubs.acs.org.

■ AUTHOR INFORMATION

Corresponding Author

*E-mail: gseelig@uw.edu.

Author Contributions

§T.J.S. and A.B.R. contributed equally to this work.

Notes

The authors declare no competing financial interest.

■ ACKNOWLEDGMENTS

We thank Michael Elowitz, Eric Klavins, Long Cai, and Mary Dunlop for their insightful comments on this manuscript. This work was supported by National Science Foundation (NSF) CAREER Award 0954566 and a Burroughs Wellcome Career Award at the Scientific Interface to GS.

■ REFERENCES

(1) Raj, A., and van Oudenaarden, A. (2008) Nature, nurture, or chance: Stochastic gene expression and its consequences. *Cell 135*, 216−226.

(2) Raj, A., Peskin, C. S., Tranchina, D., Vargas, D. Y., and Tyagi, S. (2006) Stochastic mRNA synthesis in mammalian cells. *PLoS Biol. 4*, e309.

(3) Balázsi, G., van Oudenaarden, A., and Collins, J. J. (2011) Cellular decision making and biological noise: From microbes to mammals. *Cell 144*, 910−925.

(4) Rosenfeld, N., Young, J. W., Alon, U., Swain, P. S., and Elowitz, M. B. (2005) Gene regulation at the single-cell level. *Science 307*, 1962.

(5) Pedraza, J. M., and van Oudenaarden, A. (2005) Noise propagation in gene networks. *Science 307*, 1965−1969.

(6) Carthew, R. W., and Sontheimer, E. J. (2009) Origins and mechanisms of miRNAs and siRNAs. *Cell 136*, 642−655.

(7) Ebert, M. S., and Sharp, P. A. (2012) Roles for microRNAs in conferring robustness to biological processes. *Cell 149*, 515−524.

(8) Hornstein, E., and Shomron, N. (2006) Canalization of development by microRNAs. *Nat. Genet. 38*, S20−S24.

(9) Mendell, J. T., and Olson, E. N. (2012) MicroRNAs in stress signaling and human disease. *Cell 148*, 1172−1187.

(10) Li, X., Cassidy, J. J., Reinke, C. A., Fischboeck, S., and Carthew, R. W. (2009) A microRNA imparts robustness against environmental fluctuation during development. *Cell 137*, 273−282.

(11) Chang, K., Elledge, S. J., and Hannon, G. J. (2006) Lessons from Nature: microRNA-based shRNA libraries. *Nat. Methods 3*, 707−714.

(12) Brown, B. D., Gentner, B., Cantore, A., Colleoni, S., Amendola, M., Zingale, A., Baccarini, A., Lazzari, G., Galli, C., and Naldini, L. (2007) Endogenous microRNA can be broadly exploited to regulate transgene expression according to tissue, lineage, and differentiation state. *Nat. Biotechnol. 25*, 1457−1467.

(13) Deans, T. L., Cantor, C. R., and Collins, J. J. (2007) A tunable genetic switch based on RNAi and repressor proteins for regulating gene expression in mammalian cells. *Cell 130*, 363−372.

(14) Tigges, M., Dénervaud, N., Greber, D., Stelling, J., and Fussenegger, M. (2010) A synthetic low-frequency mammalian oscillator. *Nucleic Acids Res. 38*, 2702−2711.

(15) Beisel, C. L., Bayer, T. S., Hoff, K. G., and Smolke, C. D. (2008) Model-guided design of ligand-regulated RNAi for programmable control of gene expression. *Mol. Syst. Biol. 4*, 224.

(16) Bleris, L., Xie, Z., Glass, D., Adadey, A., Sontag, E., and Benenson, Y. (2011) Synthetic incoherent feedforward circuits show adaptation to the amount of their genetic template. *Mol. Syst. Biol. 7*, 519.

(17) Xie, Z., Wroblewska, L., Prochazka, L., Weiss, R., and Benenson, Y. (2011) Multi-input RNAi-based logic circuit for identification of specific cancer cells. *Science 333*, 1307−1311.

(18) Osella, M., Bosia, C., Corá, D., and Caselle, M. (2011) The role of incoherent microRNA-mediated feedforward loops in noise buffering. *PLoS Comp. Biol. 7*, e1001101.

(19) Goentoro, L., Shoval, O., Kirschner, M. W., and Alon, U. (2009) The incoherent feedforward loop can provide fold-change detection in gene regulation. *Mol. Cell 36*, 894−899.

(20) Ma, W., Trusina, A., El-Samad, H., Lim, W. A., and Tang, C. (2009) Defining network topologies that can achieve biochemical adaptation. *Cell 138*, 760−773.

(21) Sontag, E. D. (2010) Remarks on feedforward circuits, adaptation, and pulse memory. *IET Syst. Biol. 4*, 39−51.

(22) Bosia, C., Osella, M., Baroudi, M. E., Corà, D., and Caselle, M. (2012) Gene autoregulation via intronic microRNAs and its functions. *BMC Syst. Biol. 6*, 131.

(23) Makeyev, E. V., Zhang, J., Carrasco, M. A., and Maniatis, T. (2007) The MicroRNA miR-124 promotes neuronal differentiation by triggering brain-specific alternative pre-mRNA splicing. *Mol. Cell 27*, 435−448.

(24) Karginov, F. V., Conaco, C., Xuan, Z., Schmidt, B. H., Parker, J. S., Mandel, G., and Hannon, G. J. (2007) A biochemical approach to identifying microRNA targets. *Proc. Natl. Acad. Sci. U.S.A. 104*, 19291−19296.

(25) Baccarini, A., Chauhan, H., Gardner, T. J., Jayaprakash, A. D., Sachidanandam, R., and Brown, B. D. (2011) Kinetic analysis reveals the fate of a microRNA following target regulation in mammalian cells. *Curr. Biol. 21*, 369−376.

(26) Paulsson, J. (2004) Summing up the noise in gene networks. *Nature 427*, 415−418.

(27) Nevozhay, D., Adams, R. M., Murphy, K. F., Josić, K., and Balázsi, G. (2009) Negative autoregulation linearizes the dose−response and suppresses the heterogeneity of gene expression. *Proc. Natl. Acad. Sci. U.S.A. 106*, 5123−5128.

(28) Sigal, A., Milo, R., Cohen, A., Geva-Zatorsky, N., Klein, Y., Liron, Y., Rosenfeld, N., Danon, T., Perzov, N., and Alon, U. (2006) Variability and memory of protein levels in human cells. *Nature 444*, 643−646.

(29) Ebert, M. S., Neilson, J. R., and Sharp, P. A. (2007) MicroRNA sponges: Competitive inhibitors of small RNAs in mammalian cells. *Nat. Methods 4*, 721−726.

(30) Dill, H., Linder, B., Fehr, A., and Fischer, U. (2012) Intronic miR-26b controls neuronal differentiation by repressing its host transcript, ctdsp2. *Genes Dev. 26*, 25−30.

(31) Megraw, M., Sethupathy, P., Gumireddy, K., Jensen, S. T., Huang, Q., and Hatzigeorgiou, A. G. (2010) Isoform specific gene auto-regulation via miRNAs: A case study on miR-128b and ARPP-21. *Theor. Chem. Acc. 125*, 593−598.

(32) Sun, Y., Bai, Y., Zhang, F., Wang, Y., Guo, Y., and Guo, L. (2010) miR-126 inhibits non-small cell lung cancer cells proliferation by targeting EGFL7. *Biochem. Biophys. Res. Commun. 391*, 1483−1489.

(33) Marson, A., Levine, S. S., Cole, M. F., Frampton, G. M., Brambrink, T., Johnstone, S., Guenther, M. G., Johnston, W. K., Wernig, M., and Newman, J. (2008) Connecting microRNA genes to the core transcriptional regulatory circuitry of embryonic stem cells. *Cell 134*, 521−533.

(34) O'Donnell, K. A., Wentzel, E. A., Zeller, K. I., Dang, C. V., and Mendell, J. T. (2005) c-Myc-regulated microRNAs modulate E2F1 expression. *Nature 435*, 839−843.

(35) Re, A., Corá, D., Taverna, D., and Caselle, M. (2009) Genome-wide survey of microRNA−transcription factor feed-forward regulatory circuits in human. *Mol. Biosyst. 5*, 854−867.

(36) Elowitz, M. B., Levine, A. J., Siggia, E. D., and Swain, P. S. (2002) Stochastic gene expression in a single cell. *Science 297*, 1183.

(37) Zhang, Z., Qin, Y. W., Brewer, G., and Jing, Q. (2012) MicroRNA degradation and turnover: Regulating the regulators. *Wiley Interdiscip. Rev.: RNA 3*, 593−600.

(38) Yosef, N., and Regev, A. (2011) Impulse control: Temporal dynamics in gene transcription. *Cell 144*, 886−896.
(39) Nevozhay, D., Zal, T., and Balázsi, G. (2013) Transferring a synthetic gene circuit from yeast to mammalian cells. *Nat. Comm. 4*, 1451.
(40) Broderick, J. A., Salomon, W. E., Ryder, S. P., Aronin, N., and Zamore, P. D. (2011) Argonaute protein identity and pairing geometry determine cooperativity in mammalian RNA silencing. *RNA 17*, 1858−1869.
(41) Béthune, J., Artus-Revel, C. G., and Filipowicz, W. (2012) Kinetic analysis reveals successive steps leading to miRNA-mediated silencing in mammalian cells. *EMBO Rep. 13*, 716−723.
(42) Kwon, M. J., Oh, E., Lee, S., Roh, M. R., Kim, S. E., Lee, Y., Choi, Y.-L., In, Y.-H., Park, T., and Koh, S. S. (2009) Identification of novel reference genes using multiplatform expression data and their validation for quantitative gene expression analysis. *PLoS One 4*, e6162.
(43) Koh, T.-C., Lee, Y.-Y., Chang, S.-Q., and Nissom, P. M. (2009) Identification and expression analysis of miRNAs during batch culture of HEK-293 cells. *J. Biotechnol. 140*, 149−155.
(44) Livak, K. J., and Schmittgen, T. D. (2001) Analysis of relative gene expression data using real-time quantitative PCR and the $2^{-\Delta\Delta CT}$ Method. *Methods 25*, 402−408.
(45) Raj, A., van den Bogaard, P., Rifkin, S. A., van Oudenaarden, A., and Tyagi, S. (2008) Imaging individual mRNA molecules using multiple singly labeled probes. *Nat. Methods 5*, 877−879.
(46) Rifkin, S. A. (2011) Identifying fluorescently labeled single molecules in image stacks using machine learning. *Methods Mol. Biol. 772*, 329.